Electronic Supplementary Material (ESI) for Nanoscale.

Supporting Information

Ultra-stable potassium storage and hybrid mechanism of perovskite fluoride $KFeF_3$/rGO

Shuo Wang, Fei Chen, Li-ming Zhang, Yi-xuan Li, Nai-qing Ren, Kuo Cao, Jing-chao Xiao, Chun-hua Chen*

CAS Key Laboratory of Materials for Energy Conversions, Department of Materials Science and Engineering & Collaborative Innovation Center of Suzhou Nano Science and Technology, University of Science and Technology of China, Anhui Hefei 230026, China

Corresponding authors: E-mail: cchchen@ustc.edu.cn; Phone: +86-551-63606971; Fax: (+86)551-63601592.

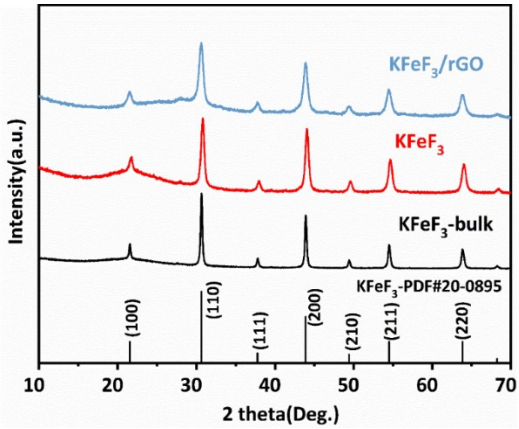

Fig. S1. XRD patterns of the obtained intermediate products after the solvothermal procedure.

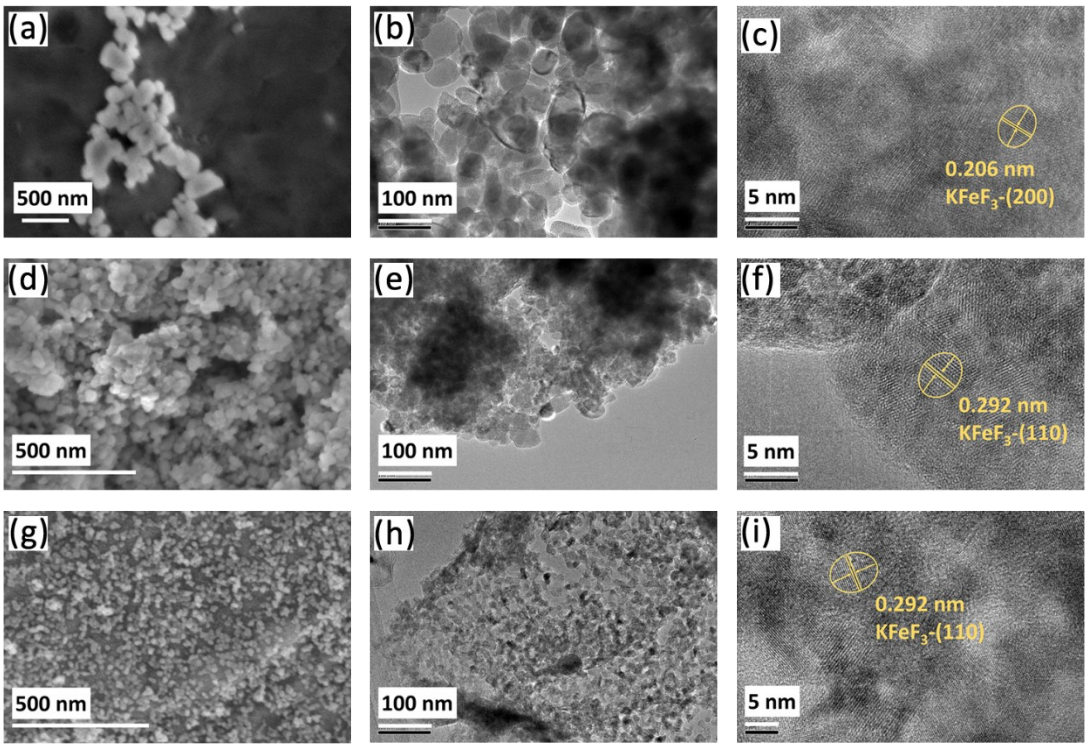

Fig. S2. The morphology characterization of the intermediate products: SEM (a), TEM (b) and HRTEM (c) images of $KFeF_3$-bulk; while (d-f) and (g-i) are corresponding to $KFeF_3$ and $KFeF_3$/GO, respectively.

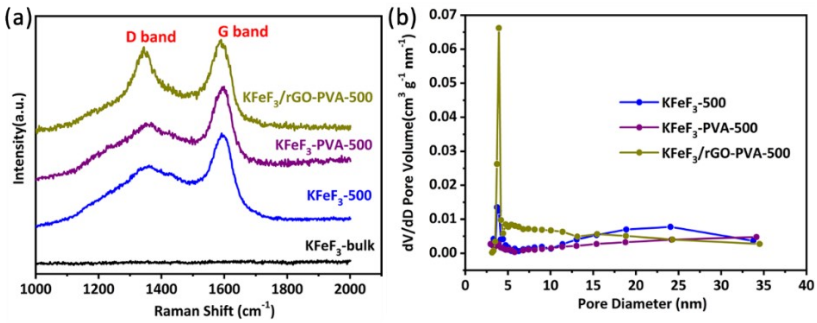

Fig. S3. Raman spectra of the samples (a) and their pore size distribution analyzed (b).

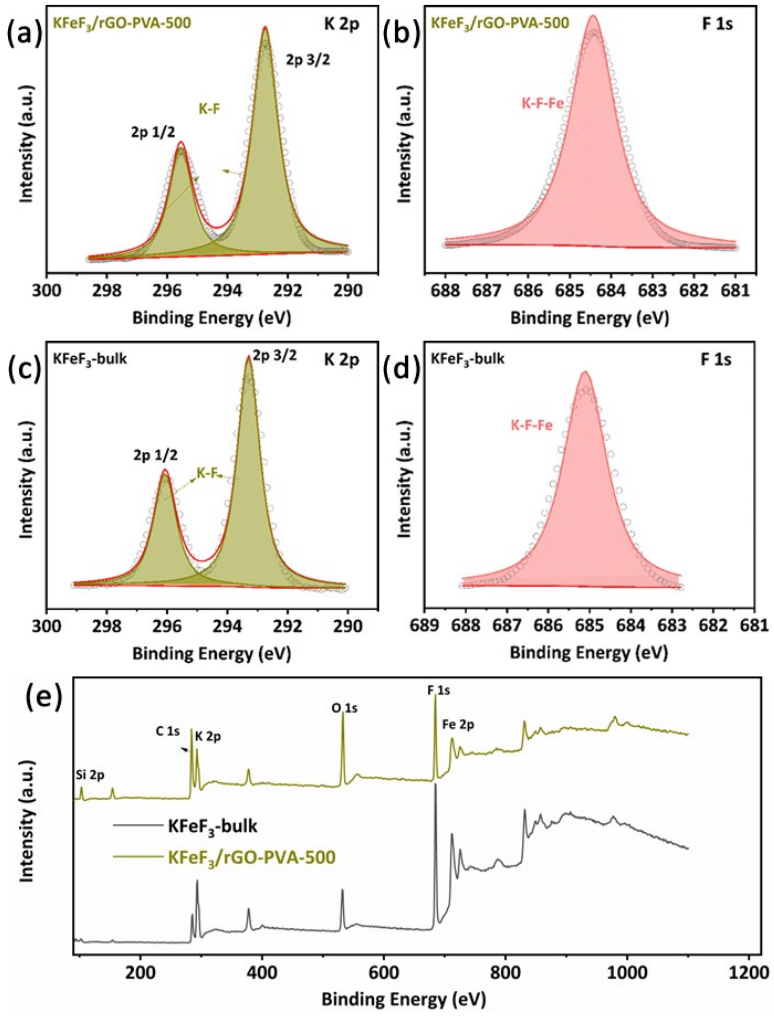

Fig. S4. XPS K 2p and F 1s spectra of $KFeF_3$/rGO-PVA-500 (a, b), $KFeF_3$-bulk (c, d) and their survey spectra (e).

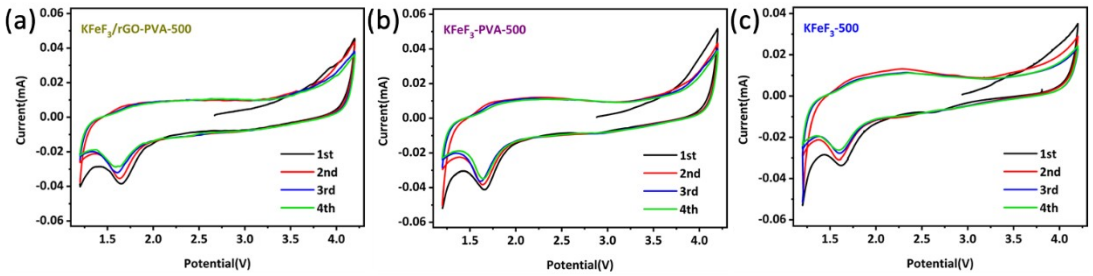

Fig. S5. The CV curves of $KFeF_3$/rGO-PVA-500 (a), $KFeF_3$-PVA-500 (b) and $KFeF_3$-500 (c) at a scan rate of 0.1 mV s^{-1}.

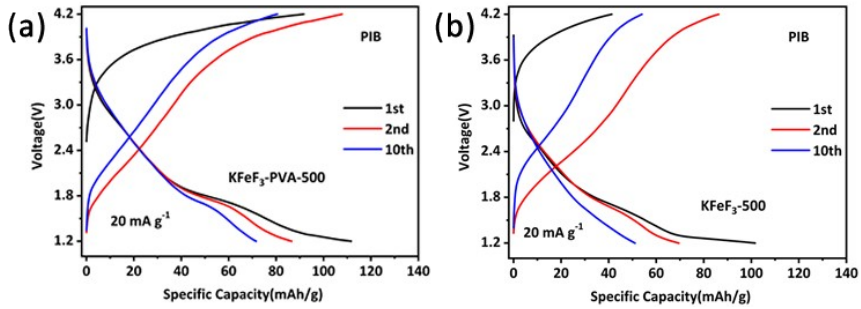

Fig. S6. The charge/discharge voltage profiles of $KFeF_3$-PVA-500 (a) and $KFeF_3$-500 (b) during the initial 3 cycles at 20 mA g^{-1}.

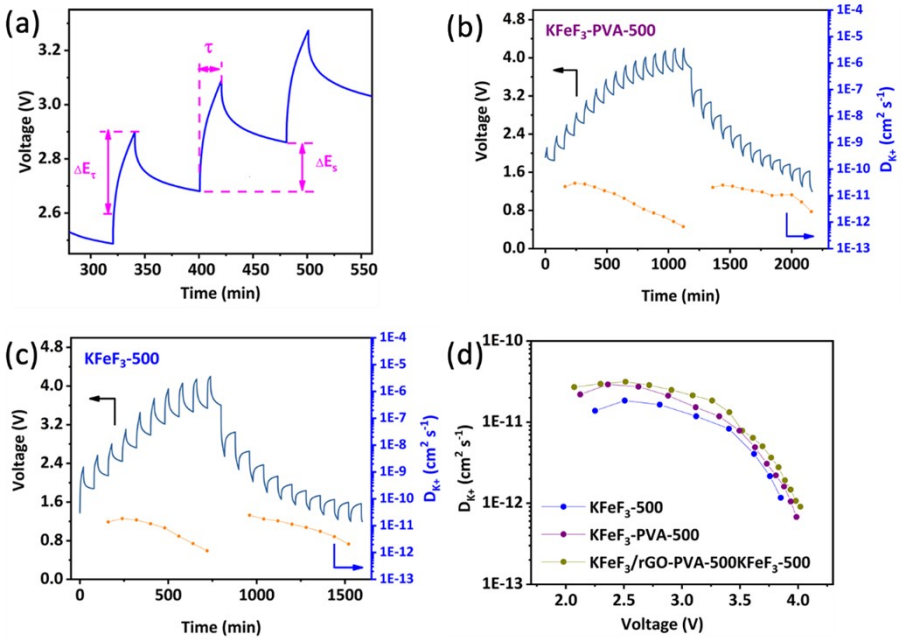

Fig. S7. The detailed schematic diagram of a single-step GITT experiment during charging (a); the GITT curves and corresponding D_{K^+} of each current pulse-relaxation step in $KFeF_3$-PVA-500 (b) and $KFeF_3$-500 (c); and the K^+ diffusion coefficient comparisons in charging process (d).

The apparent K^+ diffusion coefficients were calculated by the following equation[1]:

$$D_{K+} = \frac{4}{\pi\tau}\left(\frac{n_m V_m}{S}\right)^2\left(\frac{\Delta E_s}{\Delta E_\tau}\right)^2 \qquad \tau \ll \frac{L^2}{D_{K+}} \tag{1}$$

As shown in Figure S7a, τ, n_m, V_m and L are the duration of current pulse, the number of moles, molar volume of the active materials and the thickness of the loading slurry, respectively. ΔE_s represents the difference between the equilibrium voltages before and after the pulse. ΔE_τ is the variation of cell voltage during a titration step.

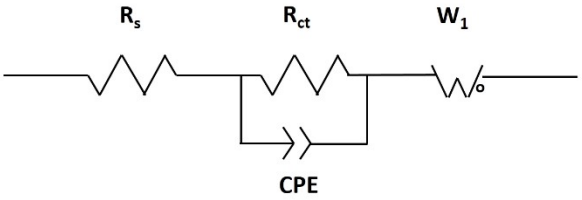

Fig. S8. The circuit model employed in EIS fitting.

Table S1. The powder electronic conductivity of the final sintered products.

sample	Powder electronic conductivity， S cm^{-1}
$KFeF_3$ -500	$<5\times10^{-6}$
$KFeF_3$ -PVA-500	$<5\times10^{-6}$
$KFeF_3$/rGO-PVA-500	4.8×10^{-2}

Table S2. The ICP results of $KFeF_3$-bulk and $KFeF_3$/rGO-PVA-500.

sample	Atomic ratio K/Fe
$KFeF_3$ -bulk	1.00
$KFeF_3$/rGO-PVA-500	0.99

Table S3. Comparison of the long cycle stability of $KFeF_3$/rGO-PVA-500 with other PIBs cathodes.

	Materials	Capacity retention	Reference
1	$KFeF_3$/KB	93%, 80 mA g^{-1}, 100th	[2]
2	Co-doped $KMnF_3$	88%, 40 mA g^{-1},60th	[3]
3	$K_{0.44}Ni_{0.22}Mn_{0.78}O_2$	67%, 200 mA g^{-1},500th	[4]
4	δ -MnO_2/$KMnF_3$	73%, 100 mA g^{-1},200th	[5]
5	O-doped $KMnF_3$@C	83%, 100 mA g^{-1},200th	[6]
6	$K_{0.83}V_2O_5$	82%, 100 mA g^{-1},200th $^{-1}$	[7]
7	$KFeF_3$/rGO-PVA-500	94%, 200 mA g^{-1},1000th	**This work**

Table S4. The ICP results of $KFeF_3$/rGO-PVA-500 at different electrochemical states.

$KFeF_3$/rGO-PVA-500	Atomic ratio K/Fe
pristine	0.99
Charged to 4.2 V	0.71
Discharged to 1.2 V	1.46

Table S5. The EIS fitting results of the samples.

sample	R_s, Ω	R_{ct}, Ω
$KFeF_3$ -500	18	3785
$KFeF_3$ -PVA-500	15	1804
$KFeF_3$/rGO-PVA-500	8	708

References:

1. W. Zhang, H. X. Li, Z. A. Zhang, M. Xu, Y. Q. Lai, S. L. Chou, Small 2020, 16, 2001524.
2. D. P. Cao, C. L. Yin, D. R. Shi, Z. W. Fu, J. C. Zhang, C. L. Li, Adv. Funct. Mater. 2017, 27, 1701130.
3. S. Y. Wang, B. Cui, Q. C. Zhuang, Y. L. Shi, H. Zheng, J. Electrochem. Soc. 2019, 166, A1819-A1826.
4. X. Zhang, Y. Yang, X. Qu, Z. Wei, G. Sun, K. Zheng, H. Yu, F. Du, Adv. Funct. Mater. 2019, 29, 1905679.
5. S. Y. Wang, Y. L. Cui, B. Cui, Q. C. Zhuang, B. Li, H. Zheng, Z. C. Ju, Adv. Mater. Interfaces 2019, 6, 1901362.
6. S. Wang, Y. Chen, B. Cui, B. Li, S. Wang, Y. Cui, Z. Ju, Q. Zhuang, Appl. Surf. Sci. 2020, 514, 145954.
7. Y. C. Zhang, X. G. Niu, L. L. Tan, L. Q. Deng, S. F. Jin, L. Zeng, H. Xu, Y. J. Zhu, ACS Appl. Mater. & Inter. 2020, 12, 9332-9340.